Supporting Information for *Acta Phys. -Chim. Sin.* doi: 10.3866/PKU.WHXB202111037

MoP-NC 纳米球负载 Pt 纳米粒子用于高效甲醇电解

李萌[1]，杨甫林[1]，常进法[2]，Alex Schechter[3]，冯立纲[1,*]

[1]扬州大学化学化工学院，江苏 扬州 225002

[2] NanoScience Technology Center, University of Central Florida, Orlando, FL 32826, USA.

[3] Department of Chemical Sciences, Ariel University, Ariel 40700, Israel.

MoP-NC Nanosphere Supported Pt Nanoparticles for Efficient Methanol Electrolysis

Meng Li [1], Fulin Yang [1], Jinfa Chang [2], Alex Schechter [3], Ligang Feng [1,*]

[1] School of Chemistry and Chemical Engineering, Yangzhou University, Yangzhou 225002, Jiangsu Province, China.

[2] NanoScience Technology Center, University of Central Florida, Orlando, FL 32826, USA.

[3] Department of Chemical Sciences, Ariel University, Ariel 40700, Israel.

[*]Corresponding author. Email: ligang.feng@yzu.edu.cn; Tel.: +86-17306299692.

Experimental

Synthesis of Pt/Mo-NC: 40 mg of Mo-NC and 333 μL H_2PtCl_6 (30 mg·mL^{-1}) were added to 50 mL of ethylene glycol with vigorous stirring. And the mixture was heated in an oil bath at 140 °C for 6 h and then cooled down naturally to room temperature. The product was washed several times with ultrapure water. Finally, the product was dried in a vacuum oven overnight and named Pt/Mo-NC.

Electrochemical measurements:

For the methanol oxidation reaction (MOR), all potentials were relative to the SCE electrode. Cyclic voltammetry was carried out at room temperature in N_2-saturated 0.5 mol·L^{-1} H_2SO_4 solution with and without 1.0 mol·L^{-1} CH_3OH solution at a potential range between −0.2 V and 1.0 V (*vs.* SCE). The electrochemical impedance spectra (EIS) were recorded at the frequency range from 1000 kHz to 10 mHz with 15 points per decade in 0.5 mol·L^{-1} H_2SO_4 with 1.0 mol·L^{-1} CH_3OH solution. The Tafel slope was calculated from the following equation: $\eta = a + b\log(j)$, where η is the overpotential (mV), b is the Tafel slope and j is the current density. It was fitted in the Tafel range. Chronoamperometry (CA) experiments were performed in 0.5 mol·L^{-1} H_2SO_4 with 1.0 mol·L^{-1} CH_3OH solution at 0.6 V for 7200 s. CO-stripping voltammetry was measured in 0.5 mol·L^{-1} H_2SO_4 solution. CO was purged into the H_2SO_4 solution for 15 minutes to allow the complete adsorption of CO onto the catalyst when the working electrode was kept at 0 V, and excess CO in the electrolyte was purged out with N_2 for 15 min. The amount of CO was evaluated by integration of the CO stripping peak, assuming 420 μC·cm^{-2} of coulombic charge required for the oxidation of the CO monolayer.

For hydrogen evolution reaction (HER), all potentials were calibrated as reversible hydrogen electrodes (RHE) by the equation: $E(\text{RHE}) = E(\text{SCE}) + 0.059\text{pH} + 0.242$ V. The catalytic performance of catalysts for HER was evaluated by linear sweep voltammograms (LSV) at a scan rate of 5 mV·s^{-1}. The Tafel slope was calculated from the following equation: $\eta = a + b\log(j)$, where η is the overpotential (mV), b is the Tafel slope and j is the current density. It was fitted in the Tafel range. Turnover frequency (TOF) values were calculated using the following equation by assuming Pt atoms in the HER as the active sites: $\text{TOF}\ (\text{s}^{-1}) = I/(2Fn)$, where I is the current (A) during linear sweep measurement, F is the Faraday's constant (96485.3 C·mol^{-1}), n is the number of active sites (mol). Because of the high catalytic nature of Pt for HER, here, Pt atoms were considered active sites for catalyzing the HER. we used a commercial 20% (*w*) Pt/C catalyst (HiSPEC™ 3000). All mass loading of Pt (0.0056 mg) in the working electrode were assumed to be active sites to evaluate the TOF. The factor 1/2 is based on the consideration that two electrons are required to produce one hydrogen molecule. The stability of the catalyst was examined through CV scanning of 1000 cycles (150 mV·s^{-1}). The EIS was recorded at the frequency range from 1000 kHz to 10 mHz and the amplitude of the sinusoidal potential signal was 5 mV. The CA experiment was tested in 0.5 mol·L^{-1} H_2SO_4 with 1.0 mol·L^{-1} CH_3OH at a constant potential (−0.03 V *vs.* RHE) for 12 h.

For two-electrode electrolysis, the ink of catalysts was used as the anode and cathode, respectively. The CV curves were tested in 0.5 mol·L^{-1} H_2SO_4 with and without 1.0 mol·L^{-1} CH_3OH at a scan rate of 5 mV·s^{-1}. CA test of the two-electrode was tested in 0.67 V for 10 h in 0.5 mol·L^{-1} H_2SO_4 with 1.0 mol·L^{-1} CH_3OH solution.

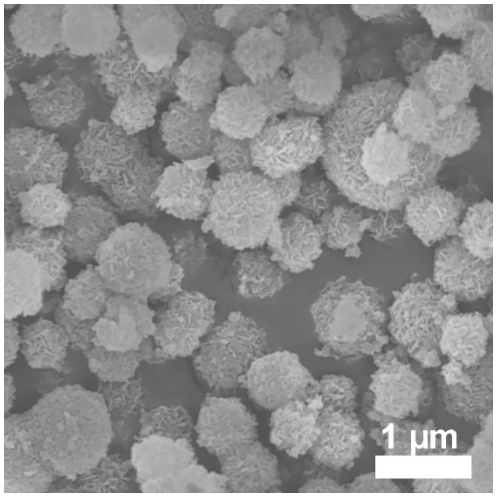

Fig. S1 SEM image of Mo-PDA.

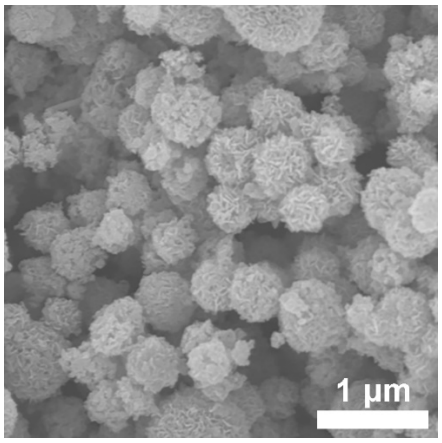

Fig. S2 SEM image of MoP-NC.

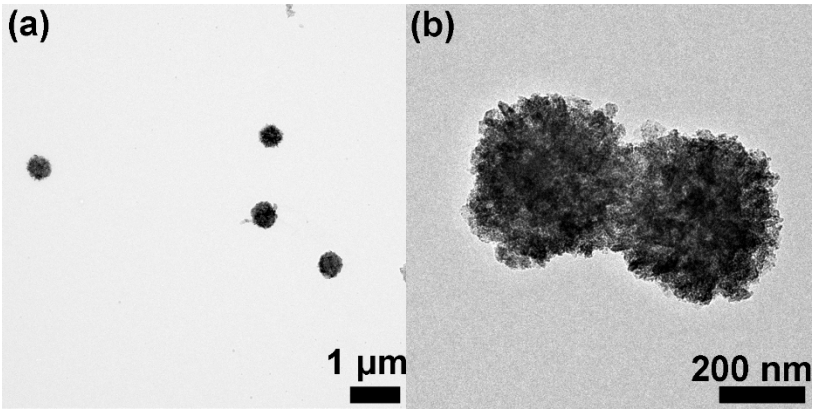

Fig. S3 TEM images of Pt/MoP-NC.

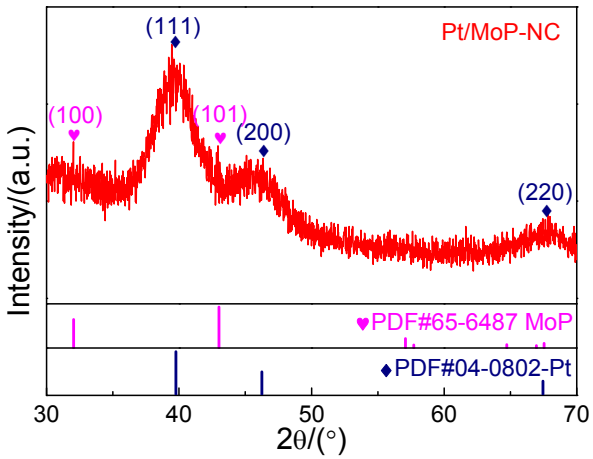

Fig. S4 X-ray diffraction pattern of Pt/MoP-NC catalysts.

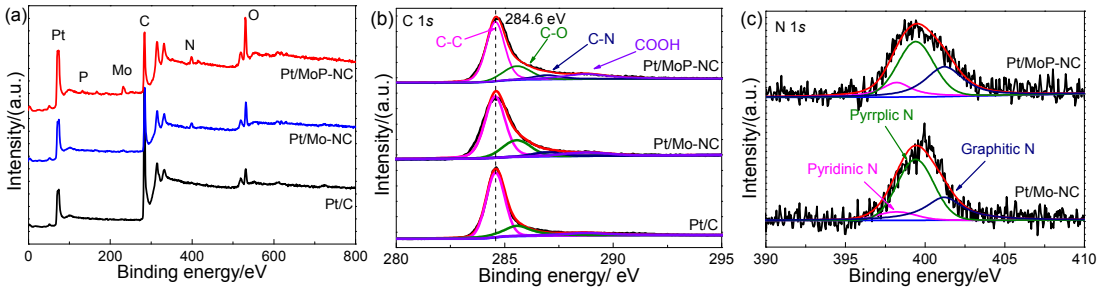

Fig. S5 XPS survey spectra (a) and high-resolution XPS spectra of C 1*s* (b), N 1*s* (c) for Pt/MoP-NC, Pt/Mo-NC and Pt/C catalysts.

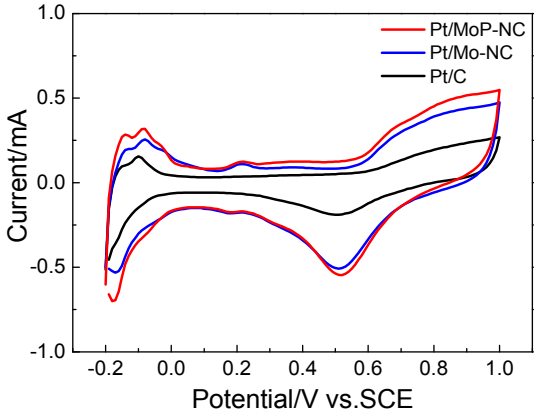

Fig. S6 CV curves of Pt/MoP-NC, Pt/Mo-NC and Pt/C catalysts in 0.5 mol·L^{-1} H_2SO_4 solution at a scan rate of 50 mV·s^{-1}.

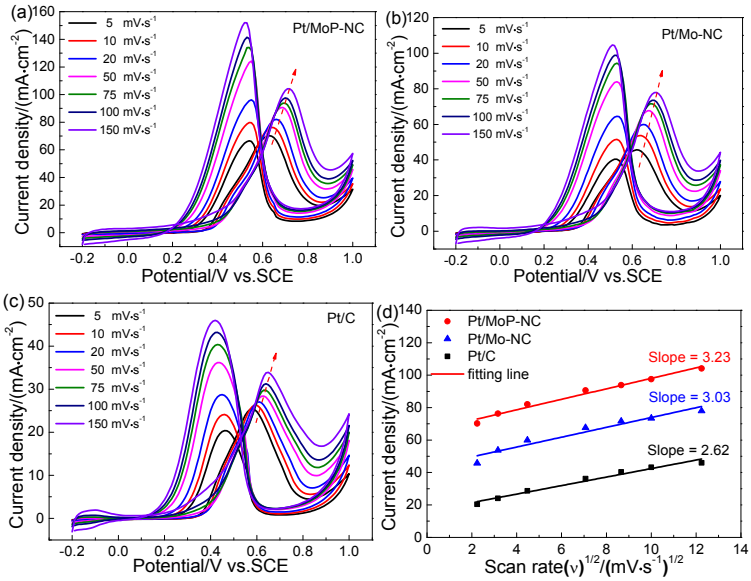

Fig. S7 Cyclic voltammograms of the (a) Pt/MoP-NC, (b) Pt/Mo-NC and (c) Pt/C catalysts in N_2-saturated 0.5 mol·L^{-1} H_2SO_4 with 1 mol·L^{-1} CH_3OH with different scan rates. (d) The plots of the anodic peak current density *vs.* the square root of scan rate.

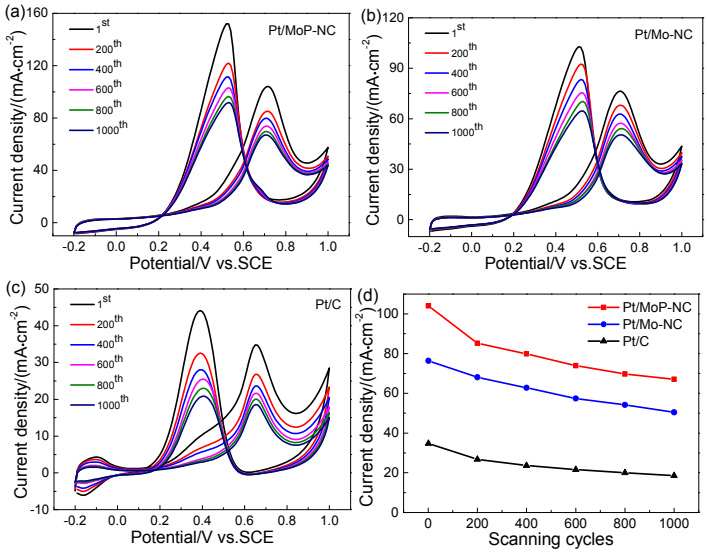

Fig. S8a The 1000 cyclic voltammograms of the (a) Pt/MoP-NC, (b) Pt/Mo-NC and (c) Pt/C catalysts in N_2-saturated 0.5 mol·L^{-1} H_2SO_4 with 1 mol·L^{-1} CH_3OH at a scan rate of 150 mV·s^{-1}. (d) Peak current density *versus* the scanning cycles for all the catalysts.

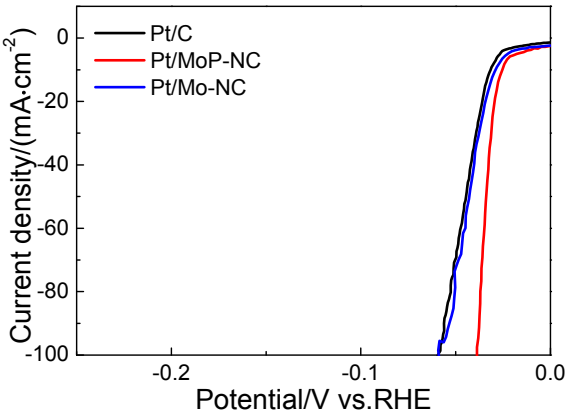

Fig. S8b Polarization curves of Pt/C, Pt/MoP-NC and Pt/Mo-NC in N_2-saturated 0.5 mol·L^{-1} H_2SO_4 with 1 mol·L^{-1} CH_3OH solution at a scan rate of 5 mV·s^{-1} with 80% *iR*-correction.

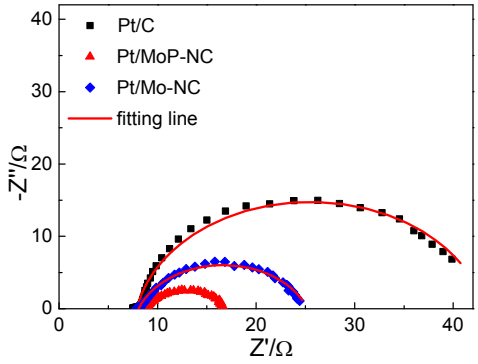

Fig. S9a Nyquist plots of the prepared electrode at the potential of −0.03 V *vs.* RHE in 0.5 mol·L^{-1} H_2SO_4 with 1.0 mol·L^{-1} CH_3OH.

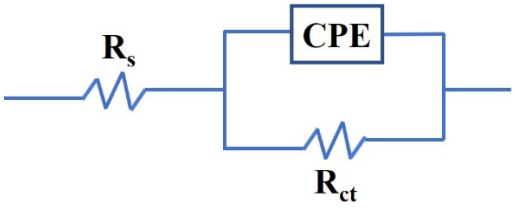

Fig. S9b An equivalent circuit diagram was used to fit the Nyquist plot. For the equivalent circuit, the R_s represents the uncompensated solution resistance; R_{ct} corresponds to the charge-transfer resistance and the constant phase element (CPE) composition is for double-layer capacitance.

Table S1 Binding energy and relative intensity of Pt species obtained from curve-fitted XPS spectra for Pt/MoP-NC, Pt/Mo-NC, and Pt/C catalysts.

Catalyst	Pt^0 (eV)		Pt^{2+} (eV)		Relative intensity (%)	
	$4f_{7/2}$	$4f_{5/2}$	$4f_{7/2}$	$4f_{5/2}$	Pt^0	Pt^{2+}
Pt/MoP-NC	71.2	74.6	72.4	75.7	69.4	30.6
Pt/Mo-NC	71.4	74.8	72.5	75.9	64.9	35.1
Pt/C	71.6	75.0	72.8	76.1	64.1	35.9

Table S2 Peak current density and onset potential for different catalyst samples for methanol oxidation.

Catalyst	Peak current density (mA·cm^{-2})	Onset potential (V *vs.* SCE)
Pt/MoP-NC	90.7	0.30
Pt/Mo-NC	67.6	0.37
Pt/C	28.5	0.41

Table S3 EIS fitting parameters from equivalent circuits for different catalyst samples in 0.5 mol·L^{-1} H_2SO_4 with 1.0 mol·L^{-1} CH_3OH.

Catalyst	R_s/Ω	CPE-Yo/(S·s^{-n})	CPE−n	R_{ct}/Ω
Pt/MoP-NC	8.2	2.5E-3	0.92	172
Pt/Mo-NC	8.3	1.9E-3	0.88	646
Pt/C	8.2	6.4E-4	0.89	1766

Table S4 Electrochemical surface area (ECSA) estimated from CO stripping experiments, the peak potential and the onset potential for CO oxidation for the relevant catalysts.

Catalyst	ECSA/(m^2·g^{-1})	Peak potential/(V *vs.* SCE)	Onset potential/(V *vs.* SCE)
Pt/MoP-NC	74.5	0.46	0.31
Pt/Mo-NC	67.5	0.51	0.37
Pt/C	57.1	0.59	0.51

Table S5 Comparisons of activities of various electrocatalysts at the peak potential for methanol oxidation in acidic media.

Catalyst	Mass activity/($mA \cdot mg_{Pt}^{-1}$)	Condition	Reference
Pt/MoP-NC	1126.58	0.5 mol·L^{-1} H_2SO_4 + 1 mol·L^{-1} CH_3OH	This work
Pt/Mo-NC	841.44	0.5 mol·L^{-1} H_2SO_4 + 1 mol·L^{-1} CH_3OH	This work
Pt/MoO_2@C	570	0.5 mol·L^{-1} H_2SO_4 + 1 mol·L^{-1} CH_3OH	1
Pt@MoS_2/NrGO	448	0.5 mol·L^{-1} H_2SO_4 + 1 mol·L^{-1} CH_3OH	2
Pt-MoO_3/RGO	610	0.5 mol·L^{-1} H_2SO_4 + 0.5 mol·L^{-1} CH_3OH	3
Pt-MoP/MWCNTs-3	1063	0.5 mol·L^{-1} H_2SO_4 + 1 mol·L^{-1} CH_3OH	4
Pt/$NiCoP_x$@NCNT-NG	867	0.5 mol·L^{-1} H_2SO_4 + 1 mol·L^{-1} CH_3OH	5
PtNW-GO	609	0.5 mol·L^{-1} H_2SO_4 + 1 mol·L^{-1} CH_3OH	6
Pt/CeO_2-P	714	0.5 mol·L^{-1} H_2SO_4 + 1 mol·L^{-1} CH_3OH	7
Pt/g-C_3N_4-CNS	832	0.5 mol·L^{-1} H_2SO_4 + 1 mol·L^{-1} CH_3OH	8
Pt/RuO_2/G	632	1 mol·L^{-1} H_2SO_4 + 2 mol·L^{-1} CH_3OH	9
PtCo CNCs	692	0.5 mol·L^{-1} H_2SO_4 + 1 mol·L^{-1} CH_3OH	10

Table S5b Comparisons of overpotential of various electrocatalysts for hydrogen evolution reaction in acidic media.

Catalyst	Condition	Overpotential ($mV \cdot mA^{-1} \cdot cm^2$)	Reference
Pt/C	0.5 mol·L^{-1} H_2SO_4 + 1 mol·L^{-1} CH_3OH	36/η_{10}	This work
Pt/MoP-NC	0.5 mol·L^{-1} H_2SO_4 + 1 mol·L^{-1} CH_3OH	30/η_{10}	This work
Pt/Mo-NC	0.5 mol·L^{-1} H_2SO_4 + 1 mol·L^{-1} CH_3OH	34/η_{10}	This work
MoP@PC	0.5 mol L^{-1} H_2SO_4	69/η_{10}	11
MoP/NG	0.5 mol L^{-1} H_2SO_4	94/η_{10}	12
$MoSe_2$/NDC	0.5 mol L^{-1} H_2SO_4	142/η_{10}	13
MoO_2/$MoSe_2$	0.5 mol L^{-1} H_2SO_4	167/η_{10}	14
MoP-Ru_2P/NPC	0.5 mol L^{-1} H_2SO_4	82/η_{10}	15
MoP/NC	0.5 mol L^{-1} H_2SO_4	183/η_{10}	16
$NiMo_{0.5}W_{0.5}O_4$	0.5 mol L^{-1} H_2SO_4	97/η_{10}	17
NiCoP/Mo_2C	0.5 mol L^{-1} H_2SO_4	116/η_{10}	18

References

(1) Zhang, J.; Sui, X.; Huang, G.; Gu, D.; Wang, Z. *J. Mater. Chem. A* **2017,** *5* (8), 4067. doi: 10.1039/c6ta09468f

(2) Ramakrishnan, S.; Karuppannan, M.; Vinothkannan, M.; Ramachandran, K.; Kwon, O. J.; Yoo, D. J. *ACS Appl. Mater. Interfaces* **2019,** *11* (13), 12504. doi: 10.1021/acsami.9b00192

(3) Hao, Y. F.; Wang, X. D.; Zheng, Y. Y.; Shen, J. F.; Yuan, J. H.; Wang, A. J.; Niu, L.; Huang, S. T. *Electrochim. Acta* **2016,** *198*, 127. doi: 10.1016/j.electacta.2016.03.054

(4) Zhou, C.; Gan, M.; Xie, F.; Ma, L.; Ding, J.; Shen, J.; Han, S.; Wei, D.; Zhan, W. *Ionics* **2020,** *26* (12), 6331. doi: 10.1007/s11581-020-03707-1

(5) Ding, J.; Hu, W.; Ma, L.; Gan, M.; Xie, F.; Zhan, W.; Lu, W. *J. Power Sources* **2021,** *481*, 228888. doi: 10.1016/j.jpowsour.2020.228888

(6) Zhao, J.; Zeng, H.; Lu, Z. *ACS Appl. Nano Mater.* **2022,** *5* (9), 13594. doi: 10.1021/acsanm.2c03358

(7) Tao, L.; Shi, Y.; Huang, Y.; Chen, R.; Zhang, Y.; Huo, J.; Zou, Y.; Yu, G.; Luo, J.; Dong, C.; *et al*. *Nano Energy* **2018,** *53*, 604. doi: 10.1016/j.nanoen.2018.09.013

(8) Liang, X.; Dong, F.; Tang, Z.; Wang, Q. *Int. J. Hydrogen Energy* **2021,** *46* (80), 39645. doi: 10.1016/j.ijhydene.2021.09.228

(9) Huang, H.; Zhu, J.; Li, D.; Shen, C.; Li, M.; Zhang, X.; Jiang, Q.; Zhang, J.; Wu, Y. *J. Mater. Chem. A* **2017,** *5* (9), 4560. doi: 10.1039/C6TA10548C

(10) Li, Z.; Jiang, X.; Wang, X.; Hu, J.; Liu, Y.; Fu, G.; Tang, Y. *Appl. Catal. B* **2020,** *277*, 119135. doi: 10.1016/j.apcatb.2020.119135

(11) Lei, Y.; Jia, M. M.; Guo, P. W.; Liu, J.; Zhai, J. Y. *Catal. Commun.* **2020,** *140*, 106000. doi: 10.1016/j.catcom.2020.106000

(12) Huang, C.; Pi, C.; Zhang, X.; Ding, K.; Qin, P.; Fu, J.; Peng, X.; Gao, B.; Chu, P. K.; Huo, K. *Small* **2018,** *14* (25), 1800667. doi: 10.1002/smll.201800667

(13) Cao, Z.; Hu, H.; Wu, M.; Tu, C.; Zhang, D.; Wu, Z. *Sustain. Energy Fuels* **2019,** *3* (9), 2409. doi: 10.1039/C9SE00311H

(14) Luo, J.; Xu, P.; Zhang, D.; Wei, L.; Zhou, D.; Xu, W.; Li, J.; Yuan, D. *Nanotechnology* **2017,** *28* (46), 465404. doi: 10.1088/1361-6528/aa8947

(15) Gao, Y.; Chen, Z.; Zhao, Y.; Yu, W.; Jiang, X.; He, M.; Li, Z.; Ma, T.; Wu, Z.; Wang, L. *Appl. Catal. B* **2022,** *303*, 120879. doi: 10.1016/j.apcatb.2021.120879

(16) Lin, M.; Lu, R.; Luo, W.; Xu, N.; Zhao, Y.; Mai, L. *ACS Appl. Energy Mater.* **2021,** *4* (6), 5486. doi: 10.1021/acsaem.1c00121

(17) Kasturi, P. R.; Shanmugapriya, S.; Elizabeth, M.; Athira, K.; Selvan, R. K. *J. Mater. Sci.: Mater. Electron.* **2020,** *31* (3), 2378. doi: 10.1007/s10854-019-02773-0

(18) Wang, Y.; Wang, B.; Chu, W.; Kong, Y.; Wu, Q.; Liu, Z. *Int. J. Hydrogen Energy* **2020,** *45* (53), 28774. doi: 10.1016/j.ijhydene.2020.07.232